

Proceedings of “Applications of Physics in Mechanical and Material Engineering” (APMME 2023)

The Influence of Medium Movement on the Occurrence of Band Gaps in Quasi Two Dimensional Phononic Crystals

S. GARUS^{a,*}, W. SOCHACKI^a AND J. RZAŃKI^b

^a*Department of Mechanics and Fundamentals of Machinery Design, Faculty of Mechanical Engineering and Computer Science, Czestochowa University of Technology, Dąbrowskiego 73, 42-201 Czestochowa, Poland*

^b*Department of Physics, Faculty of Production Engineering and Materials Technology, Czestochowa University of Technology, Dąbrowskiego 73, 42-201 Czestochowa, Poland*

Doi: [10.12693/APhysPolA.144.284](https://doi.org/10.12693/APhysPolA.144.284)

*e-mail: sebastian.garus@pcz.pl

Phononic quasi-two-dimensional structures, due to their properties, namely the lack of propagation of selected frequency ranges of the mechanical wave, can be used as filters of acoustic waves. In the paper, an analysis of the propagation of mechanical waves in these highly dispersive structures in the conditions of a moving medium was carried out. The influence of the number of metaatom layers on the transmission of a mechanical wave for different medium velocities was analysed.

topics: phononic crystal, finite-difference time domain (FDTD), moving medium, band gaps

1. Introduction

Research on sound propagation in periodic structures and the formation of band gaps in phononic crystals is conducted by many research centers around the world. These are works in which the authors, apart from describing the formation of the band gap [1, 2], point to the practical application of this phenomenon in periodic structures. They therefore indicate the possibility of using phononic crystals as acoustic wave filters [3–6], waveguides [7] or acoustic diodes [8]. These studies most often concern cases of sound propagation without movement of the medium in which the sound propagates.

However, taking into account that the speed of sound is only about 34–110 times higher than typical wind speeds in the atmosphere, it should be assumed that wind and turbulence in the atmosphere have a significant impact on sound propagation.

Among the many methods that can be used to describe this issue, such as the curved ray tracing method [9] or the transmission-line matrix method (TLM) [10], the most promising is the finite-difference time domain (FDTD) method. The use of the FDTD method to describe the propagation of acoustic waves in a moving medium is the subject of many works. In [11], the authors proposed two sets of differential equations to describe the propagation of sound in a moving atmosphere. The sound propagation in a moving medium for the case when the typical speed of movement in the

medium is slightly lower than the speed of wave propagation through the medium was the subject of work [12]. In turn, works [13, 14] present two-dimensional FDTD calculations for the atmosphere, taking into account the influence of motion (wind and turbulence) in the propagation medium, as well as the interaction with the ground. Extensive literature on a wide range of issues related to the linear propagation of sound in a moving medium is presented in the review article [15].

Using a finite-difference algorithm in the time domain, the work analyzed the influence of medium motion on the propagation and transmission of mechanical waves in quasi-two-dimensional phononic structures with various numbers of layers.

2. Finite difference time domain algorithm for a moving medium

The propagation of a mechanical wave in a moving medium is described by a system of first-order differential equations

$$\frac{\partial p}{\partial t} = -\kappa \nabla \cdot \mathbf{w}, \quad (1)$$

$$\frac{\partial \mathbf{w}}{\partial t} = -b \nabla p, \quad (2)$$

which for the two-dimensional case gives

$$\frac{\partial p}{\partial t} = -\kappa \left(\frac{\partial w_x}{\partial x} + \frac{\partial w_y}{\partial y} \right), \quad (3)$$

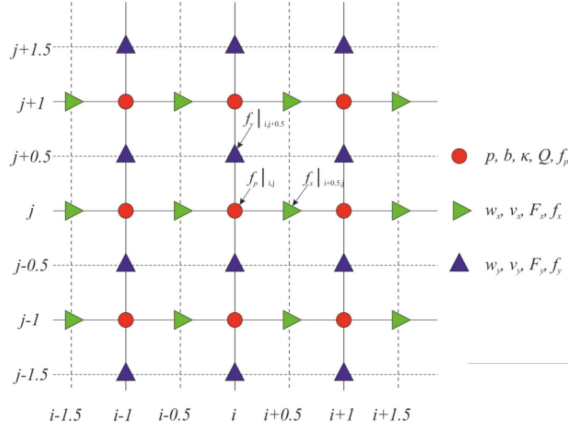


Fig. 1. Spatially staggered finite-difference grid used for the calculations.

$$\frac{\partial w_x}{\partial t} = -b \frac{\partial p}{\partial x}, \quad (4)$$

$$\frac{\partial w_y}{\partial t} = -b \frac{\partial p}{\partial y}, \quad (5)$$

where p is the acoustic pressure, \mathbf{w} is the acoustic particle velocity, t is the time. The adiabatic bulk modulus κ [$\frac{\text{kg}}{\text{m}^3 \text{s}^2}$] is defined by

$$\kappa = \rho c^2, \quad (6)$$

and the mass buoyancy b is defined by

$$b = 1/\rho, \quad (7)$$

where ρ is the ambient medium density, and c is the adiabatic speed of sound.

Assuming that the sound wave causes slight disturbances in the medium, there is no turbulence of the background velocity field, and due to the consideration of sound propagation near the ground, the background pressure gradient is omitted and the medium is adiabatic. Then the propagation of a mechanical wave in a moving medium is described by

$$\frac{\partial p}{\partial t} = -(\mathbf{v} \cdot \nabla) p - \rho c^2 \nabla \cdot \mathbf{w} + \rho c^2 Q, \quad (8)$$

$$\frac{\partial \mathbf{w}}{\partial t} = -(\mathbf{w} \cdot \nabla) \mathbf{v} - (\mathbf{v} \cdot \nabla) \mathbf{w} - \frac{\nabla p}{\rho} + \frac{\mathbf{F}}{\rho}. \quad (9)$$

In equations (8) and (9), \mathbf{v} is the wind velocity. The sources are represented as \mathbf{F} (a force acting on the medium — dipole pressure source) and Q (mass source — monopole pressure source).

Equations (8) and (9) for the two-dimensional case gives

$$\frac{\partial p}{\partial t} = -\left(v_x \frac{\partial p}{\partial x} + v_y \frac{\partial p}{\partial y}\right) - \kappa \left(\frac{\partial w_x}{\partial x} + \frac{\partial w_y}{\partial y}\right) + \kappa Q, \quad (10)$$

$$\begin{aligned} \frac{\partial w_x}{\partial t} = & -\left(w_x \frac{\partial v_x}{\partial x} + w_y \frac{\partial v_x}{\partial y}\right) - \left(v_x \frac{\partial w_x}{\partial x} + v_y \frac{\partial w_x}{\partial y}\right) \\ & - b \frac{\partial p}{\partial x} + b F_x, \end{aligned} \quad (11)$$

$$\begin{aligned} \frac{\partial w_y}{\partial t} = & -\left(w_x \frac{\partial v_y}{\partial x} + w_y \frac{\partial v_y}{\partial y}\right) - \left(v_x \frac{\partial w_y}{\partial x} + v_y \frac{\partial w_y}{\partial y}\right) \\ & - b \frac{\partial p}{\partial y} + b F_y. \end{aligned} \quad (12)$$

Figure 1 shows the grid used in the calculations. The spatial coordinates x and y are determined from the product of the appropriate node coordinates i and j and the appropriate grid spacings Δx and Δy by

$$(x, y) = (i\Delta x, j\Delta y). \quad (13)$$

The pressure p is stored in the nodes with the integer values of variables i and j , just like the values of b , κ , Q and the component f_p . The non-integer nodes store the horizontal and vertical components of \mathbf{w} , \mathbf{v} and \mathbf{F} .

In order to take into account the division of time and space, the notation $p|_{i,j}^n$ was introduced, where for the pressure p the coefficients “ i ”, “ j ” mean a simplified notation of the position in space, which in full form is defined by $i\Delta x$ and $j\Delta y$, respectively, while “ n ” is a simplified notation of the moment $n\Delta t$ in time, where Δt is the value of a single time step.

Expanding the derivatives into appropriate differences and assuming that $\Delta x = \Delta y$, equations (10)–(12) take the form

$$\begin{aligned} \frac{\partial}{\partial t} p|_{i,j}^n = & -\frac{1}{4\Delta x} \left(v_x|_{i+0.5,j}^n + v_x|_{i-0.5,j}^n\right) \left(p|_{i+1,j}^n - p|_{i-1,j}^n\right) - \frac{1}{4\Delta x} \left(v_y|_{i,j+0.5}^n + v_y|_{i,j-0.5}^n\right) \left(p|_{i,j+1}^n - p|_{i,j-1}^n\right) \\ & - \frac{\kappa|_{i,j}^n}{\Delta x} \left(w_x|_{i+0.5,j}^n - w_x|_{i-0.5,j}^n + w_y|_{i,j+0.5}^n - w_y|_{i,j-0.5}^n\right) + \kappa|_{i,j}^n Q|_{i,j}^n, \end{aligned} \quad (14)$$

$$\begin{aligned} \frac{\partial}{\partial t} w_x|_{i+0.5,j}^n = & -\frac{w_x|_{i+0.5,j}^n}{2\Delta x} \left(v_x|_{i+1.5,j}^n - v_x|_{i-0.5,j}^n\right) - \frac{v_x|_{i+0.5,j}^n}{2\Delta x} \left(w_x|_{i+1.5,j}^n - w_x|_{i-0.5,j}^n\right) \\ & - \frac{v_x|_{i+0.5,j+1}^n - v_x|_{i+0.5,j-1}^n}{8\Delta y} \left(w_y|_{i+1,j+0.5}^n + w_y|_{i,j+0.5}^n + w_y|_{i+1,j-0.5}^n + w_y|_{i,j-0.5}^n\right) \\ & - \frac{w_x|_{i+0.5,j+1}^n - w_x|_{i+0.5,j-1}^n}{8\Delta y} \left(v_y|_{i+1,j+0.5}^n + v_y|_{i,j+0.5}^n + v_y|_{i+1,j-0.5}^n + v_y|_{i,j-0.5}^n\right) \\ & - \frac{1}{2\Delta x} \left(b|_{i+1,j}^n + b|_{i,j}^n\right) \left(p|_{i+1,j}^n - p|_{i,j}^n\right) + \frac{b|_{i+1,j}^n + b|_{i,j}^n}{2} F_x|_{i+0.5,j}^n, \end{aligned} \quad (15)$$

$$\begin{aligned}
\frac{\partial}{\partial t} w_y|_{i,j+0.5}^n &= -\frac{w_y|_{i,j+0.5}^n}{2\Delta x} \left(v_y|_{i,j+1.5}^n - v_y|_{i,j-0.5}^n \right) - \frac{v_y|_{i,j+0.5}^n}{2\Delta x} \left(w_y|_{i,j+1.5}^n - w_y|_{i,j-0.5}^n \right) \\
&\quad - \frac{v_y|_{i+1,j+0.5}^n - v_y|_{i-1,j+0.5}^n}{8\Delta x} \left(w_x|_{i+0.5,j+1}^n + w_x|_{i+0.5,j}^n + w_x|_{i-0.5,j+1}^n + w_x|_{i-0.5,j}^n \right) \\
&\quad - \frac{w_y|_{i+1,j+0.5}^n - w_y|_{i-1,j+0.5}^n}{8\Delta x} \left(v_x|_{i+0.5,j+1}^n + v_x|_{i+0.5,j}^n + v_x|_{i-0.5,j+1}^n + v_x|_{i-0.5,j}^n \right) \\
&\quad - \frac{1}{2\Delta x} \left(b|_{i,j+1}^n + b|_{i,j}^n \right) \left(p|_{i,j+1}^n - p|_{i,j}^n \right) + \frac{b|_{i,j+1}^n + b|_{i,j}^n}{2} F_y|_{i,j+0.5}^n. \tag{16}
\end{aligned}$$

In order to simplify the notation, the functions $f_p|_{i,j}^n$, $f_x|_{i+0.5,j}^n$ and $f_y|_{i,j+0.5}^n$ are defined, respectively, as

$$\begin{aligned}
f_p|_{i,j}^n &= -\frac{1}{4\Delta x} \left(v_x|_{i+0.5,j}^n + v_x|_{i-0.5,j}^n \right) \left(p|_{i+1,j}^n - p|_{i-1,j}^n \right) \\
&\quad - \frac{1}{4\Delta x} \left(v_y|_{i,j+0.5}^n + v_y|_{i,j-0.5}^n \right) \left(p|_{i,j+1}^n - p|_{i,j-1}^n \right) \\
&\quad - \frac{\kappa|_{i,j}^n}{\Delta x} \left(w_x|_{i+0.5,j}^n - w_x|_{i-0.5,j}^n + w_y|_{i,j+0.5}^n - w_y|_{i,j-0.5}^n \right) \\
&\quad + \kappa|_{i,j}^n Q|_{i,j}^n, \tag{17}
\end{aligned}$$

$$\begin{aligned}
f_x|_{i+0.5,j}^n &= -\frac{w_x|_{i+0.5,j}^n}{2\Delta x} \left(v_x|_{i+1.5,j}^n - v_x|_{i-0.5,j}^n \right) \\
&\quad - \frac{v_x|_{i+0.5,j+1}^n - v_x|_{i+0.5,j-1}^n}{8\Delta x} \left(w_y|_{i+1,j+0.5}^n + w_y|_{i,j+0.5}^n \right. \\
&\quad \left. + w_y|_{i+1,j-0.5}^n + w_y|_{i,j-0.5}^n \right) \\
&\quad - \frac{v_x|_{i+0.5,j}^n}{2\Delta x} \left(w_x|_{i+1.5,j}^n - w_x|_{i-0.5,j}^n \right) \\
&\quad - \frac{w_x|_{i+0.5,j+1}^n - w_x|_{i+0.5,j-1}^n}{8\Delta x} \left(v_y|_{i+1,j+0.5}^n + v_y|_{i,j+0.5}^n \right. \\
&\quad \left. + v_y|_{i+1,j-0.5}^n + v_y|_{i,j-0.5}^n \right) + \frac{b|_{i+1,j}^n + b|_{i,j}^n}{2} F_x|_{i+0.5,j}^n \\
&\quad - \frac{1}{2\Delta x} \left(b|_{i+1,j}^n + b|_{i,j}^n \right) \left(p|_{i+1,j}^n - p|_{i,j}^n \right), \tag{18}
\end{aligned}$$

and

$$\begin{aligned}
f_y|_{i,j+0.5}^n &= -\frac{v_y|_{i+1,j+0.5}^n - v_y|_{i-1,j+0.5}^n}{8\Delta x} \left(w_x|_{i+0.5,j+1}^n \right. \\
&\quad \left. + w_x|_{i+0.5,j}^n + w_x|_{i-0.5,j+1}^n + w_x|_{i-0.5,j}^n \right) \\
&\quad - \frac{w_y|_{i,j+0.5}^n}{2\Delta x} \left(v_y|_{i,j+1.5}^n - v_y|_{i,j-0.5}^n \right) \\
&\quad - \frac{w_y|_{i+1,j+0.5}^n - w_y|_{i-1,j+0.5}^n}{8\Delta x} \left(v_x|_{i+0.5,j+1}^n + v_x|_{i+0.5,j}^n \right. \\
&\quad \left. + v_x|_{i-0.5,j+1}^n + v_x|_{i-0.5,j}^n \right) + \frac{b|_{i,j+1}^n + b|_{i,j}^n}{2} F_y|_{i,j+0.5}^n \\
&\quad - \frac{v_y|_{i,j+0.5}^n}{2\Delta x} \left(w_y|_{i,j+1.5}^n - w_y|_{i,j-0.5}^n \right) \\
&\quad - \frac{1}{2\Delta x} \left(b|_{i,j+1}^n + b|_{i,j}^n \right) \left(p|_{i,j+1}^n - p|_{i,j}^n \right). \tag{19}
\end{aligned}$$

Using (17)–(19), the equations (14)–(16) with the iteratively previous time step proceeding Δt take the form

$$p|_{i,j}^{n+1/2} = p|_{i,j}^{n-1/2} + \Delta t f_p|_{i,j}^{n-1/2}, \tag{20}$$

$$w_x|_{i+0.5,j}^n = w_x|_{i+0.5,j}^{n-1} + \Delta t f_x|_{i+0.5,j}^{n-1}, \tag{21}$$

$$w_y|_{i,j+0.5}^n = w_y|_{i,j+0.5}^{n-1} + \Delta t f_y|_{i,j+0.5}^{n-1}. \tag{22}$$

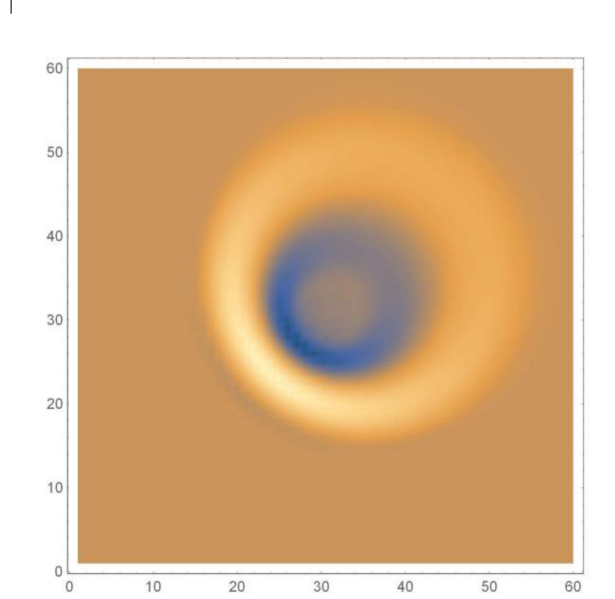


Fig. 2. The influence of wind on the propagation of the sound wave.

Figure 2 shows the pressure distribution for a propagating Gaussian pulse after 3000 time steps in air. The movement of the medium in both horizontal and vertical directions is taken into account. As can be seen, a wave propagating in the direction opposite to the wind decreases in length and at the same time increases in amplitude. An increase in wavelength and a decrease in amplitude occurs when the wind direction and the direction of wave propagation match.

3. Research

The work analyzed the propagation of a Gaussian pulse from a soft wave source marked with point ‘‘S’’ in Fig. 3 through a regular structure composed of metaatoms with a square cross-section and a lattice constant of 2 cm and a fill factor of 68.75%.

The spatial step Δx was 0.125 m, and the time step Δt ensuring simulation stability was 100 times smaller than that resulting from the Courant stability condition for two-dimensional analysis and amounted to 2.6×10^{-6} s. Two sizes of structures

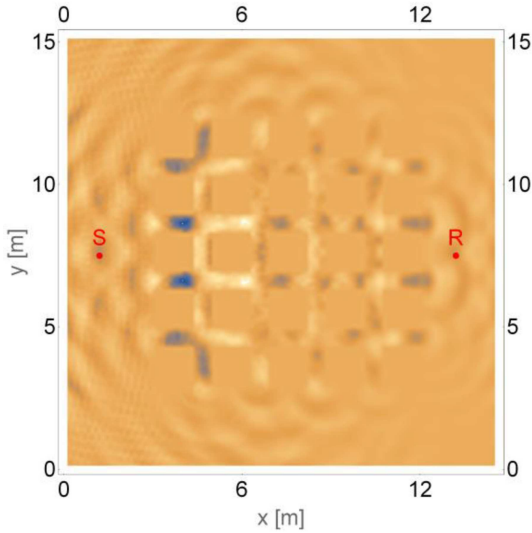


Fig. 3. Pressure distribution for 2×10^4 time steps of impulse propagation in a 5-by-5 structure for the medium velocity $v_x = 60$ m/s.

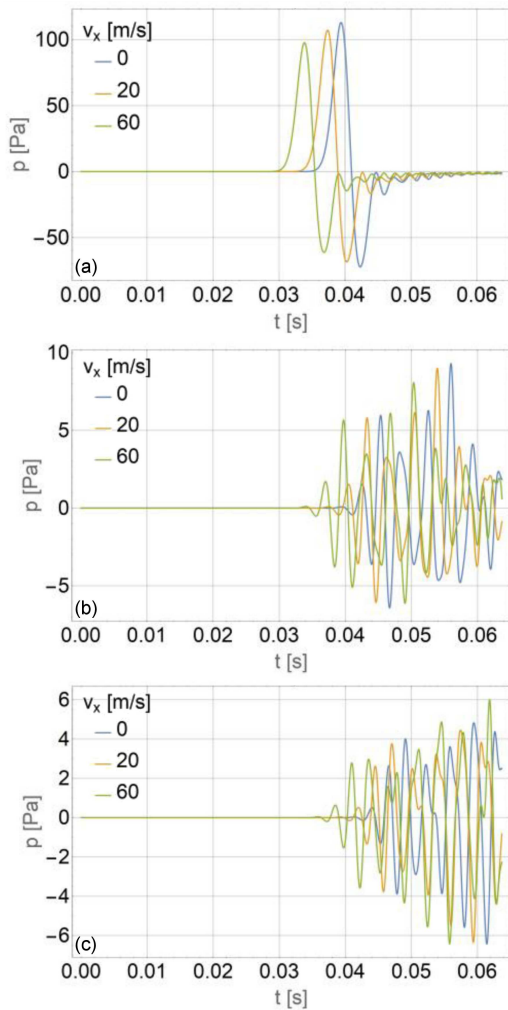


Fig. 4. Pressure time series collected at point R (a) with no structure, (b) for the 3-by-5 structure, and (c) for the 5-by-5 structure for different values of the medium velocity v_x .

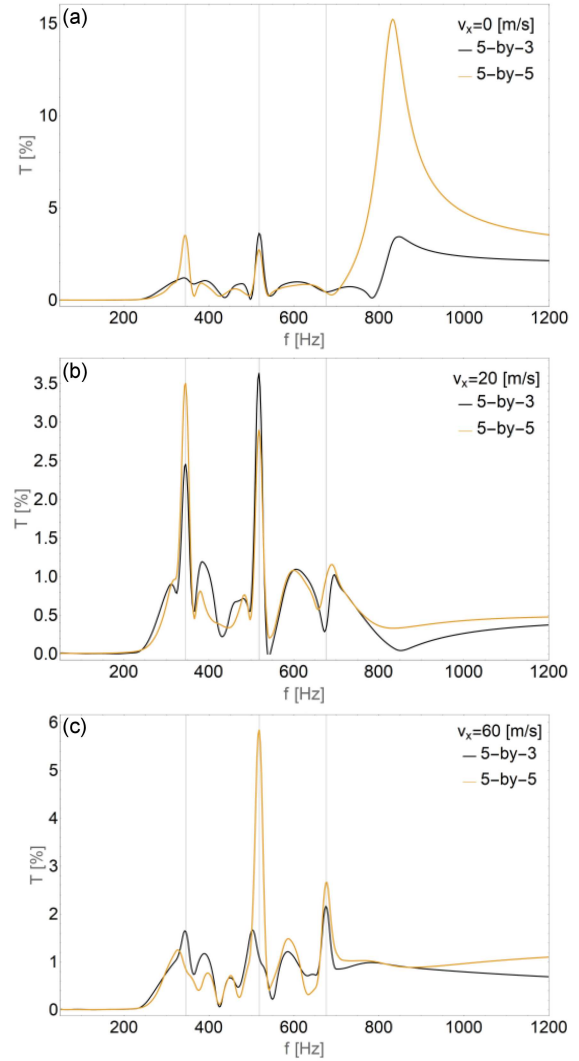


Fig. 5. Wave transmission at point R for different values of the medium velocity (a) $v_x = 0$ m/s, (b) $v_x = 20$ m/s and (c) $v_x = 60$ m/s.

were analyzed in this study. The first one is 3 columns of 5 rows (3-by-5), and the second one is 5 columns of 5 rows (5-by-5). In order to determine the transmission, a study of the propagation of a wave pulse in a space without structures was also carried out. The wave propagated in the air and the metaatoms were simulated as a rigid wall.

At the point marked “R” in Fig. 3, the time series of pressure changes presented for the analyzed cases in Fig. 4 were recorded. As shown in Fig. 4, the velocity of the medium in the direction of wave propagation shortened the time for the wavefront to reach the receiver point R. The presence of the phononic structure caused the wave to slow down and significantly reduce its intensity the greater the number of layers in the structure.

Figure 5 shows transmission graphs for various medium velocities and structure sizes. The tests carried out showed the occurrence of transmission peaks whose frequency (345 Hz and 519 Hz) was

independent of the speed of the medium. The intensity of the peaks changed with the velocity of the medium. These peaks were associated with the emerging areas of local resonances inside the intermetaatomic spaces. The high-intensity peak occurring in the absence of medium movement at 832 Hz, with the increase in the v_x velocity, moved towards lower frequencies (676 Hz for $v_x = 60$ m/s) while decreasing its energy, which was related to the increase in the wavelength due to the coincidence of the medium movement speed with the direction of wave propagation.

4. Conclusions

The work analyzed the influence of the motion of the medium on the propagation and transmission of a mechanical wave through a quasi-two-dimensional phononic structure composed of metaatoms with a square cross-section.

An increase in the propagation speed of the mechanical wave was demonstrated when the direction of the medium's velocity was consistent with it. The phononic structure caused the wave propagation to slow down, the greater the number of layers it consisted of. The formation of transmission peaks was demonstrated as a result of the formation of local resonance areas in the intermetaatomic space, the intensity of which was influenced by the velocity of the medium. The occurrence of a peak was demonstrated, the frequency of which decreased with the increase in the velocity of the medium.

References

- [1] W. Witarto, K.B. Nakshatrala, Y-L. Mo, *Mech. Mater.* **134**, 38 (2019).
- [2] S-L. Cheng, J-M. Liang, Q. Ding, Q. Yan, Y-T. Sun, T-J. Xin, L. Wang, *Wave Motion* **122**, 103195 (2023).
- [3] C.J. Rupp, M.L. Dunn, K. Maute, *Appl. Phys. Lett.* **96**, 111902 (2010).
- [4] S. Villa-Arango, R. Torres, P.A. Kyriacou, R. Lucklum, *Measurement* **102**, 20 (2017).
- [5] W. Sochacki, *Acta Phys. Pol. A* **138** 328 (2020).
- [6] S. Garus, W. Sochacki, *Wave Motion* **98**, 102645 (2020).
- [7] B. Morvan, A. Tinel, J.O. Vasseur, R. Sainidou, P. Rembert, A.-C. Hladky-Hennion, N. Swintek, P.A. Deymier, *J. Appl. Phys.* **116**, 214901 (2014).
- [8] X.-F. Li, X. Ni, L. Feng, M.-H. Lu, C. He, Y.-F. Chen, *Phys. Rev. Lett.* **106**, 084301 (2011).
- [9] Q. Mo, H. Yeh, M. Lin, D. Manocha, *Appl. Acoust.* **104**, 142 (2016).
- [10] Q. Goestchel, G. Guillaume, D. Ecotiere, B. Gauvreau, *J. Sound Vib.* **531**, 116974 (2022).
- [11] V.E. Ostashev, D.K. Wilson, L. Liu, D.F. Aldridge, N.P. Symons, D. Marlin, *J. Acoust. Soc. Am.* **117**, 2(2005).
- [12] D.K. Wilson, L. Liu, *Engineer Research and Development Center, Cold Regions Research and Engineering Laboratory*, ERDC/CRREL TR-04-12, 2004.
- [13] R. Blumrich, D. Heimann, *J. Acoust. Soc. Am.* **112**, 446 (2002).
- [14] E.M. Salomons, R. Blumrich, D. Heimann, *Acta Acust. united Ac.* **88**, 483 (2002).
- [15] T. Van Renterghem, *Int. J. Aeroacoust.* **13**, 385 (2014).